PHYSICAL REVIEW B **96**, 140501(R) (2017)

Pressure-induced half-collapsed-tetragonal phase in $CaKFe_4As_4$

Udhara S. Kaluarachchi,[1,2] Valentin Taufour,[2,*] Aashish Sapkota,[1,2] Vladislav Borisov,[3] Tai Kong,[1,2,†] William R. Meier,[1,2] Karunakar Kothapalli,[2] Benjamin G. Ueland,[2] Andreas Kreyssig,[1,2] Roser Valentí,[3] Robert J. McQueeney,[1,2] Alan I. Goldman,[1,2] Sergey L. Bud'ko,[1,2] and Paul C. Canfield[1,2]

[1]*Department of Physics and Astronomy, Iowa State University, Ames, Iowa 50011, USA*

[2]*Ames Laboratory, U.S. DOE, Iowa State University, Ames, Iowa 50011, USA*

[3]*Institute of Theoretical Physics, Goethe University Frankfurt am Main, D-60438 Frankfurt am Main, Germany*

(Received 21 February 2017; revised manuscript received 20 June 2017; published 2 October 2017)

We report the temperature-pressure phase diagram of $CaKFe_4As_4$ established using high-pressure electrical resistivity, magnetization, and high-energy x-ray diffraction measurements up to 6 GPa. With increasing pressure, both resistivity and magnetization data show that the bulk superconducting transition of $CaKFe_4As_4$ is suppressed and then disappears at $p \gtrsim 4$ GPa. High-pressure x-ray data clearly indicate a phase transition to a collapsed tetragonal phase in $CaKFe_4As_4$ under pressure that coincides with the abrupt loss of bulk superconductivity near 4 GPa. The x-ray data, combined with resistivity data, indicate that the collapsed tetragonal transition line is essentially independent of pressure, occurring at 4.0(5) GPa for temperatures below 150 K. Density functional theory calculations also find a sudden transition to a collapsed tetragonal state near 4 GPa, as As-As bonding develops across the Ca layer. Bonding across the K layer only occurs for $p \geqslant 12$ GPa. These findings demonstrate a different type of collapsed tetragonal phase in $CaKFe_4As_4$ as compared to $CaFe_2As_2$: a half-collapsed tetragonal phase.

DOI: 10.1103/PhysRevB.96.140501

The discovery of superconductivity in FeAs-based compounds [1–4] opened a new chapter in high-temperature superconductor research. Among them the $AEFe_2As_2$ (AE=alkaline earth), so-called 122 systems, gained attention [5,6] due to the ease of growing large, high-quality, single crystals and the relative simplicity of the structure. At ambient pressure, the parent compounds adopt the $ThCr_2Si_2$-type structure and, in most cases, undergo structural and magnetic transitions upon lowering of the temperature [5,6]. Application of pressure or chemical doping generally suppresses the structural/magnetic transitions and reveals superconductivity [5–12]. Although chemical substitution is an effective way to alter the lattice parameters and the density of states at the Fermi energy, it also introduces disorder that can effect the physics in uncontrollable ways. Therefore physical pressure is one of the cleaner ways to perturb these systems and understand their intertwined and competing phase transitions.

The Ca^{2+} ionic radius in Ca122 [5,13,14] is the smallest of the AE122 family and Ca122 is exceptionally sensitive to pressure [5,7,15,16]. Application of less than 0.5 GPa pressure suppresses the first-order structural/magnetic transition and reveals a transition to a nonmagnetic, collapsed-tetragonal phase [5,7,15,16]. In contrast, at ambient pressure K122 shows superconductivity with a relatively low T_c [17–19] without any structural/magnetic transition. The effect of pressure on K122 has attracted attention due to the unusual "V-shaped" [20–22] pressure dependence of T_c with a minimum in T_c near 1.8 GPa. At higher pressures, a collapsed-tetragonal phase was observed for $p \geqslant 16$ GPa at room temperature [23–26].

Recently, a new superconductor with a related structure, $CaAFe_4As_4$ (A=K,Rb,Cs), was discovered by Iyo *et al.* [27]. Unlike a $(Ca_{1-x}K_x)122$ [28] solid solution, which has the $I4/mmm$ body-centered-tetragonal space group, $CaKFe_4As_4$ [27,29] has separate, unique crystallographic sites for the alkaline and alkaline-earth-metal atoms, and possesses in the primitive tetragonal $P4/mmm$ space group. At ambient pressure, $CaKFe_4As_4$ shows bulk superconductivity below $T_c \sim 35$ K in zero applied field or below 700 kOe $\leqslant Hc_2 \leqslant$ 900 kOe at low temperatures [29]. Initial pressure work up to $\sim$4 GPa [29] has shown that T_c is suppressed to 28.5 K by 3.9 GPa. To further determine and understand the p-T phase diagram of this system, higher-pressure studies are needed.

In this Rapid Communication we present resistivity, magnetization, and structural measurements of $CaKFe_4As_4$ under pressures up to 6 GPa and find a half-collapsed-tetragonal (hcT) phase stabilized for $p \gtrsim 4$ GPa. Above this pressure there is an $\approx$2.6% decrease in the c-axis lattice parameter and an $\approx$0.4% increase in the a-lattice parameter. This hcT phase transition coincides with the abrupt loss of bulk superconductivity in the magnetization and the resistance measurements. A similar collapsed-tetragonal phase is observed under pressure in both $CaFe_2As_2$ and KFe_2As_2. In the case of $CaFe_2As_2$, it is not superconducting even before the collapsed-tetragonal (cT) transition. However, relatively low $T_c \sim 3$ K of KFe_2As_2 at ambient pressure is killed by the cT transition. In the present case, $T_c \sim 35$ K in the superconducting phase, and this relatively high-T_c superconductivity is killed by the hcT. Density functional theory (DFT) calculations show that, for $p \gtrsim 4$ GPa, As-As bonding takes place across the Ca layer with much higher pressures needed to cause such bonding to span the larger K layer. Taken together, $CaKFe_4As_4$ undergoes a simultaneous structural collapse and loss of superconductivity with As-As bond formation across the Ca but not the K layers.

$CaKFe_4As_4$ single crystals were grown using the high-temperature solution growth technique described in Refs. [29,30]. Temperature-dependent magnetization and resistance were carried out using a Quantum Design (QD) Magnetic Property Measurement System and a QD Physical

*Present address: Department of Physics, University of California, Davis, California 95616, USA.

†Present address: Department of Chemistry, Princeton University, Princeton, NJ 08544, USA.

Property Measurement System, respectively. The ac resistivity was measured by the standard four-probe method with the current in the ab plane. Four Pt wires, with diameters of 25 μm, were soldered to the sample using a Sn:Pb–60:40 alloy. For the resistivity measurements, pressure was applied at room temperature using a modified Bridgman cell [31] with a 1:1 mixture of n-pentane:isopentane as a pressure medium [32]. The pressure was determined at low temperature by monitoring the superconducting transition temperature of Pb [33,34]. High-pressure magnetization measurements were carried out using a moissanite anvil cell [35] with Daphne 7474 as a pressure medium [36]. The pressure was applied at room temperature and the ruby fluorescence technique [37] at 77 K was used to determine the pressure (see Supplemental Material [38] for further details).

High-energy x-ray-diffraction measurements were performed on a six-circle diffractometer at end station 6-ID-D at the Advanced Photon Source, using an x-ray energy of $E = 100.33$ keV and a beam size of $100 \times 100\ \mu m^2$. Single-crystal samples were loaded into a double-membrane-driven [39] copper-beryllium diamond-anvil cell (DAC). Helium was used as the pressure-transmitting medium and loaded to a pressure of 0.7 GPa at 300 K. Ruby spheres and silver foil were also mounted in the DAC for pressure determination. The DAC was attached to the cold finger of a He closed-cycle refrigerator. Diffraction patterns were recorded using a MAR345 image plate detector positioned at 1.494 m from the sample position. The distance was determined from measurement of powder patterns of a CeO_2 standard from the National Institute of Standards and Technology. The detector was operated with a pixel size of $100 \times 100\ \mu m^2$, and patterns were recorded while rocking the sample through two independent angles up to $\pm 3.6^\circ$ about the axes perpendicular to the incident beam. The measurement was performed in the (H, K, H) scattering plane [38].

In order to investigate the electronic and structural properties of $CaKFe_4As_4$, we performed DFT relativistic calculations using the Vienna *ab initio* Simulation Package (VASP) [40–42] with the projector-augmented wave basis [43,44] in the generalized-gradient approximation. In order to take into account, in the first approximation, the paramagnetic fluctuations that preserve the tetragonal symmetry of the lattice ($a = b$), we consider a model with a "frozen", twisted, long-range magnetic order which is one of the lowest-energy configurations with this symmetry. Pressure-dependent structures were obtained by fixing the components of the stress tensor to the given value (equal to the external pressure) and fully relaxing the lattice parameters and the internal atomic positions with the conjugate-gradient method [45–47]. The integration over the irreducible Brillouin zone was realized on the Γ-centered $(10 \times 10 \times 10)$ k mesh [38].

Figures 1(a) and 1(b) show the zero-field-cooled (ZFC) magnetization data, $M(T)$, on single-rystalline samples of $CaKFe_4As_4$ under pressure below 40 K. These data have been normalized to the ZFC data of a larger sample at ambient pressure [29]. The low field $M(T)$ data in Fig. 1(a) show a clear diamagnetic signal below T_c. T_c monotonically decreases with the pressure up to 3.9 GPa. Upon further increase of pressure, there is a broader and reduced diamagnetic anomaly below 20 K. The appearance of a small diamagnetic signal above 3.9 GPa can be related to nonbulk/filamentary superconductivity and can often be easily eliminated by the application of a small (1000 Oe $\ll H_{c2}$) [29] magnetic field [Fig. 1(b)] where the observation of a clear diamagnetic signal can be found only up to 3.9 GPa. This suggests nonbulk superconductivity for pressures above 3.9 GPa.

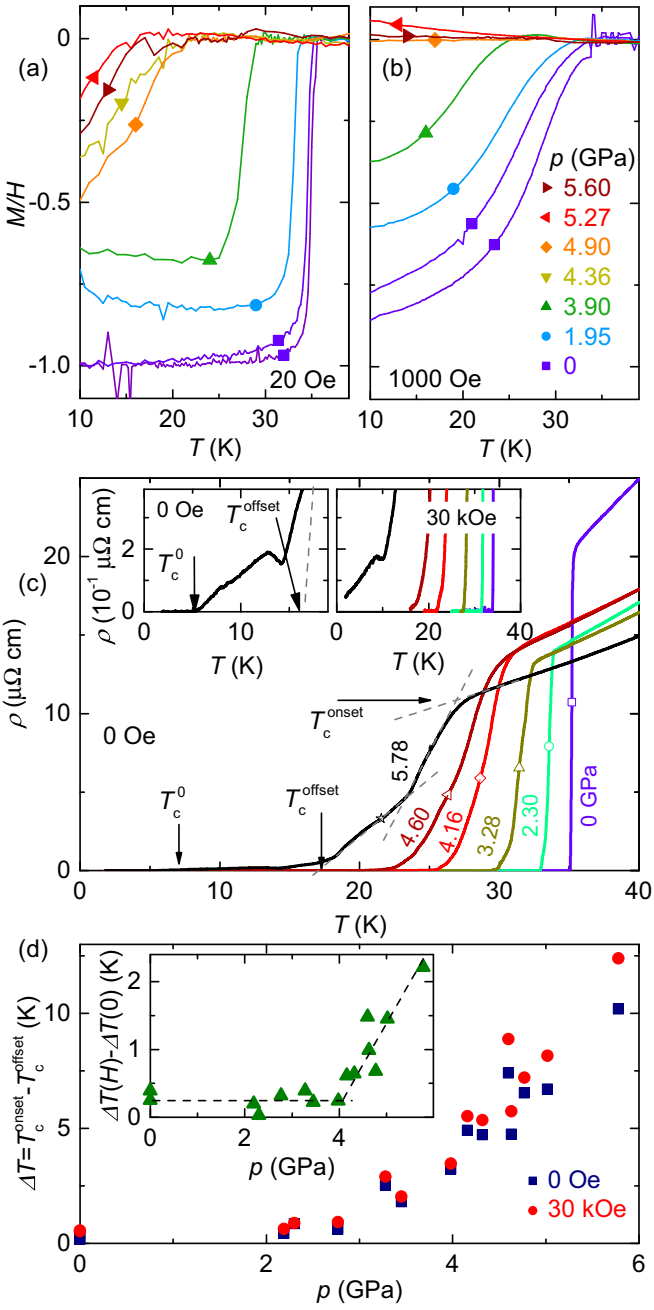

FIG. 1. The ZFC $M(T)$ data for (a) 20 Oe and (b) 1000 Oe applied fields. (c) The temperature-dependent resistivity at representative pressures. Arrows for the 5.78 GPa curve indicate T_c^{onset}, T_c^{offset}, and T_c^0 criteria used in this Rapid Communication. The left and right insets show the temperature-dependent resistivity under pressure for 0 Oe and 30 kOe applied fields, respectively. (d) Superconducting transition widths, $\Delta T = T_c^{onset} - T_c^{offset}$, for 0 and 30 kOe. The inset shows the difference of transition width, $\Delta T(H) - \Delta T(0)$, where $\Delta T(H)$ is the transition width at 30 kOe

A similar decrease in the superconducting transition temperature is observed in the resistivity measurements under pressure [Fig. 1(c)]. The sharp superconducting transition found at low pressures becomes broadened at higher pressures. The superconducting transition temperature is parametrized by three different criteria, T_c^{onset}, T_c^{offset}, and T_c^0 as shown by the arrows in Fig. 1(c) and its insets. In contrast to the loss of superconducting signature in $M(T)$, $\rho(T)$ shows zero resistivity up to 5.78 GPa. This is due to the fact that resistivity measurements are known to be more susceptible to filamentary superconductivity, thus, application of a magnetic field helps to separate it from bulk superconductivity. The left and right insets of Fig. 1(c) show the temperature-dependent resistivity under pressure for 0 Oe and 30 kOe fields. The clear observation of nonzero resistivity at 5.78 GPa at 30 kOe again confirms the nonbulk nature of the higher pressure superconductivity.

In order to determine the transition from bulk to nonbulk superconductivity in the electrical resistivity data we focus on the transition widths. The superconducting transition width, $\Delta T = T_c^{onset} - T_c^{offset}$, is broadened with the increase of pressure as illustrated by Fig. 1(d), but this can be, in part, due to pressure inhomogeneities in the pressure medium, rather than represent any sort of phase transition. In order to search for a possible transition we compare zero field and moderate, but finite field ($H = 30$ kOe $\ll H_{c2}$) resistive transition width data. Any broadening due to inhomogeneous pressure should be equally present in the $H = 0$ Oe and $H = 30$ kOe data. To determine the field contribution of the transition width, we calculated the difference of the transition widths, $\Delta T(H) - \Delta T(0)$ [inset of Fig. 1(d)]. $\Delta T(H) - \Delta T(0)$ remains constant until near 4 GPa and then starts to increase significantly for pressures above that. This critical pressure is consistent with the pressure at which the magnetization data shows a loss of bulk superconductivity. Although broadening of the superconducting transition in field can be also due to the thermal fluctuation of the vortex system, the observation, in magnetization data, of a loss of diamagnetic signal at 1000 Oe eliminates this possibility.

The data in Fig. 1 can be summarized in a pressure dependence of T_c phase diagram as shown in Fig. 2. The solid and open symbols represent the bulk and nonbulk superconductivity. Bulk superconductivity persists up to a critical pressure of $\sim$4 GPa. The faint signatures of superconductivity appearing above 4 GPa in this phase diagram are due to strain-induced, filamentary superconductivity. The sudden and discontinuous disappearance of superconductivity for $p \geqslant 4$ GPa is very suggestive of what is found for $Ca(Fe_{1-x}Co_x)_2As_2$ both as a function of x [48] and as a function of p [49], i.e., superconductivity suddenly and discontinuously disappears when a collapsed tetragonal, nonmagnetic phase is stabilized.

To further pursue these findings, we examined the pressure dependence of the lattice parameters from the diffraction study for temperatures near 130 K [Fig. 3(a)]. We observed an abrupt enhancement of the a-lattice parameter simultaneous to a significant reduction of the c-lattice parameter near 4 GPa without any crystallographic symmetry change. This indicates a pressure-induced phase transition from a tetragonal to a collapsed-tetragonal phase, similar to the observation in other 122 systems [15,23,24,50–56]. The change of the a-lattice parameter is about $\approx$0.016 Å(0.4%), while the c-lattice parameter decreases by $\approx$0.31 Å(2.6%) (raw data are shown in Fig. S1 in the Supplemental Material [38]). For both $CaFe_2As_2$ and KFe_2As_2 the c-lattice parameter decreases by $\approx$1 Å(8.6%) [15,23] at the fully collapsed state. This value is much larger than the $CaKFe_4As_4$.

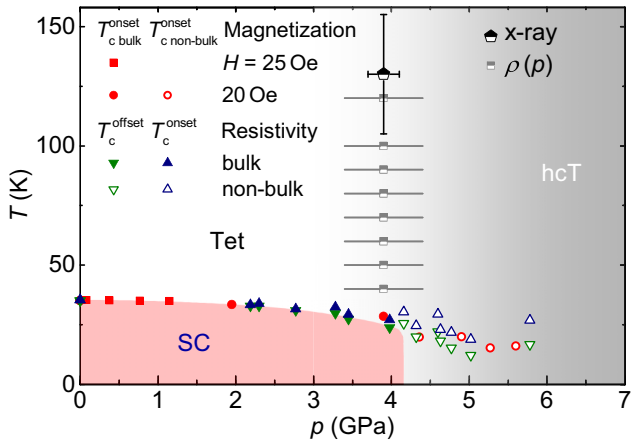

FIG. 2. Temperature-pressure phase diagram of $CaKFe_4As_4$, constructed from magnetization, resistivity, and x-ray-diffraction measurements under pressure. Solid and opened symbols represent T_c for bulk and filamentary superconductivity, respectively. Red square symbols are from Ref. [29]. The green and blue data represent T_c^{offset} and T_c^{onset}, respectively. The light-red shaded area represents the bulk superconductivity region. Half-filled pentagon and squares represent the data from high-pressure x-ray diffraction and the resistivity anomaly as seen in Figs. 3(a) and 4.

DFT calculations manifest a very similar expansion in a of $\approx$0.015 Å(0.4%), while c drops by $\approx$0.17 Å(1.5%) at the critical pressure of 4 GPa as shown in Fig. 3(b). As can be seen in Fig. 2, this collapsed-tetragonal transition point is positioned directly above the disappearance of bulk superconductivity at lower temperatures.

An analysis of the orbital-resolved band structures at different pressures near this transition confirms its collapsed nature [38]. The As antibonding molecular orbitals shift above the Fermi energy upon crossing 4 GPa (Fig. S4 in the Supplemental Material [38]). This is in accordance with a jumplike reduction of the As-As bond length across the Ca layer by $\sim$0.05 Å [Fig. 3(c)] and an increase in the As-4p_z electron density between the two As ions (Fig. S4 in the Supplemental Material [38]). A second collapse associated with As-As bonding across the K layer is found for $p \sim 12$ GPa [38]. The transition at $\sim$4 GPa then is associated with a hcT phase. Similar effects in the As-4p_z bands were observed in $CaFe_2As_2$ at the collapsed phase and further study of the second half-collapse might be promising in view of the qualitatively different high-pressure behavior of the pure KFe_2As_2 compound, compared to the $CaFe_2As_2$.

Whereas our scattering data point is for $T = 130(25)$ K, the DFT calculations are formally for $T = 0$ K and our T_c data is for $T \sim 30$ K. This begs the question of whether a half-collapsed-tetragonal phase line can be detected for $p \sim$ 4 GPa below 150 K. Figures 4(a) and 4(b) show temperature-

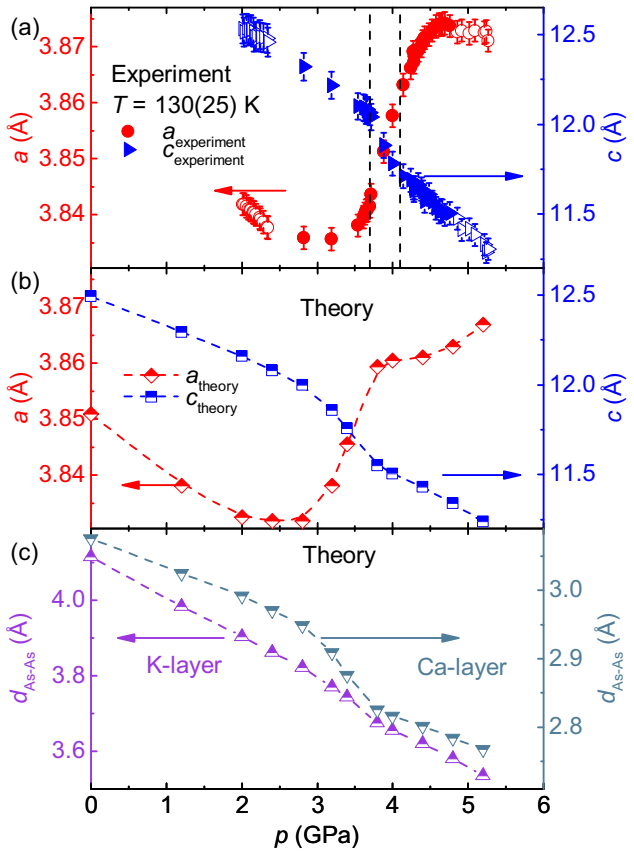

FIG. 3. (a) Pressure-dependent a- (left axis) and c- (right axis) lattice parameters obtained from the high-pressure x-ray-diffraction study. The solid symbols represent the data measured within the temperature range of 130(25) K and open symbols are for higher or lower temperature than this range. The lattice parameters are obtained after fitting the one-dimensional (0,2,0) and (1,0,1) peaks. The one-dimensional peak is obtained from a two-dimensional pattern after selecting the region of interest around the peak and integrating azimuthally. The dashed-vertical lines mark the bound of the transition and represent the error bar in Fig. 2. (b) Theoretical a- (left axis) and c- (right axis) lattice parameters represented with the same scale as (a). (c) Change of the As-As distances across the K (left axis) and Ca (right axis) cationic layers under the transition to the collapsed tetragonal phase. Dashed lines are guides for the eye.

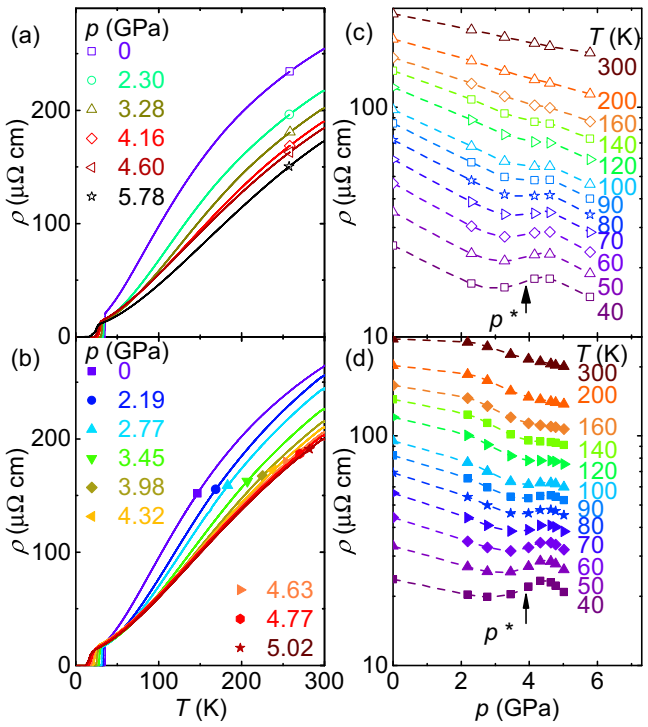

FIG. 4. (a),(b) Evolution of the temperature-dependent resistivity of $CaKFe_4As_4$ with pressure for two samples. (c), (d) Pressure dependence of resistivity at fixed temperature for the same two samples. The arrow indicates the observed resistivity anomaly at p^*.

dependent resistivity, under various pressures, data sets measured from 300 to 1.8 K. At ambient pressure $CaKFe_4As_4$ shows metallic behavior and becomes superconducting below 35 K. With increase of pressure, the resistivity at room temperature monotonically decreases up to 5.6 GPa. However, the resistivity data at lower temperature, in the normal state ($\geqslant$40 K), show a nonmonotonic pressure evolution. No clear anomaly is visible in the temperature-dependent resistivity, suggesting that any phase transition line will be near vertical as shown in Fig. 2. To see this transition line more clearly, we plotted resistivity vs pressure at fixed temperatures [Figs. 4(c) and 4(d)]. At higher temperatures, the resistivity monotonically decreases with pressure. However, below 160 K we see a jump in resistivity developing near $p^* \sim 4$ GPa. This can be related to the collapsed tetragonal phase transition as seen in high-pressure x-ray measurement. Similar features in the resistivity have been observed in K122 [25] with no clear features in $\rho(T)$ data, but V-shape minimum in $\rho(p)$.

The composite p-T phase diagram of $CaKFe_4As_4$ is shown in Fig. 2. The $p^*(T)$ data inferred from Figs. 4(c) and 4(d) [p^* being midpoint of rise in $\rho(p)$ data and error bars being width of rise] clearly links the higher-temperature x-ray data to the lower-temperature loss of superconductivity and the $T = 0$ DFT results. Figure 2 shows that the transition of Tet $\rightarrow$ hcT is nearly vertical.

To summarize, the bulk superconducting transition temperature of tetragonal $CaKFe_4As_4$ is gradually suppressed under pressure up to $\sim$4 GPa and then discontinuously disappears. High-pressure x-ray measurements combined with DFT calculations identify the phase transition from a tetragonal to a half-collapsed tetragonal phase near 4 GPa. From the diffraction study at 130 K, we find an abrupt enhancement in the a-lattice parameter (0.4%) and a reduction in the c-lattice parameter (2.6%) near 4 GPa. A reduction of the c-lattice parameter in Ca122 and K122 is much higher (8.6%) than the $CaKFe_4As_4$ (2.6%), and this provides additional evidence for the half-collapsed scenario. Specifically, with As-As bond formation across the Ca layer, but not the K layer. Indeed, DFT calculations show that the first collapse occurs across the Ca layer near 4 GPa followed by a second collapse, across the K layer, at higher pressures. Both transitions are accompanied by the typical enhancement of the corresponding As-As bonding; although, only half of the As-As bonding is collapsing at 4 GPa, when the superconducting state is fully suppressed.

We would like to acknowledge discussions with Peter Hirschfeld, Rafael Fernandes, Milan Tomić, and Wageesha Jayasekara. We thank Daniel Guterding for providing a code [57] to generate the As-4p_z electron density maps from the Wannier function analysis, and D. S. Robinson for support during the x-ray experiments. Experimental work was supported by the U.S. Department of Energy (DOE), Office of Science, Basic Energy Sciences, Materials Science and Engineering Division and was performed at the Ames Laboratory, which is operated for the U.S. DOE by Iowa State University under Contract No. DE-AC02-07CH11358. W.R.M. was supported by the Gordon and Betty Moore Foundations EPiQS Initiative through Grant No. GBMF4411. V.T. is supported by Ames Laboratory's laboratory-directed research and development (LDRD) funding for magnetization measurements under pressure. This research used resources of the Advanced Photon Source, a U.S. Department of Energy (DOE) Office of Science User Facility operated for the DOE Office of Science by Argonne National Laboratory under Contract No. DE-AC02-06CH11357. The theoretical work was financially supported by the German Research Foundation (Deutsche Forschungsgemeinschaft) through Grant No. SFB/TR49. The computer time was allotted by the Center for Supercomputing (CSC) in Frankfurt.

[1] Y. Kamihara, T. Watanabe, M. Hirano, and H. Hosono, J. Am. Chem. Soc. **130**, 3296 (2008).
[2] Z.-A. Ren, G.-C. Che, X.-L. Dong, J. Yang, W. Lu, W. Yi, X.-L. Shen, Z.-C. Li, L.-L. Sun, F. Zhou, and Z.-X. Zhao, Europhys. Lett. **83**, 17002 (2008).
[3] M. Rotter, M. Tegel, and D. Johrendt, Phys. Rev. Lett. **101**, 107006 (2008).
[4] H. Takahashi, K. Igawa, K. Arii, Y. Kamihara, M. Hirano, and H. Hosono, Nature (London) **453**, 376 (2008).
[5] P. C. Canfield and S. L. Bud'ko, Annu. Rev. Condens. Matter Phys. **1**, 27 (2010).
[6] N. Ni and S. L. Bud'ko, MRS Bull. **36**, 620 (2011).
[7] M. S. Torikachvili, S. L. Bud'ko, N. Ni, and P. C. Canfield, Phys. Rev. Lett. **101**, 057006 (2008).
[8] M. S. Torikachvili, S. L. Bud'ko, N. Ni, and P. C. Canfield, Phys. Rev. B **78**, 104527 (2008).
[9] P. L. Alireza, Y. T. C. Ko, J. Gillett, C. M. Petrone, J. M. Cole, G. G. Lonzarich, and S. E. Sebastian, J. Phys.: Condens. Matter **21**, 012208 (2009).
[10] S. A. J. Kimber, A. Kreyssig, Y.-Z. Zhang, H. O. Jeschke, R. Valenti, F. Yokaichiya, E. Colombier, J. Yan, T. C. Hansen, T. Chatterji, R. J. McQueeney, P. C. Canfield, A. I. Goldman, and D. N. Argyriou, Nat. Mater. **8**, 471 (2009).
[11] E. Colombier, S. L. Bud'ko, N. Ni, and P. C. Canfield, Phys. Rev. B **79**, 224518 (2009).
[12] A. S. Sefat, Rep. Prog. Phys. **74**, 124502 (2011).
[13] N. Ni, S. Nandi, A. Kreyssig, A. I. Goldman, E. D. Mun, S. L. Bud'ko, and P. C. Canfield, Phys. Rev. B **78**, 014523 (2008).
[14] F. Ronning, T. Klimczuk, E. D. Bauer, H. Volz, and J. D. Thompson, J. Phys.: Condens. Matter **20**, 322201 (2008).
[15] A. Kreyssig, M. A. Green, Y. Lee, G. D. Samolyuk, P. Zajdel, J. W. Lynn, S. L. Bud'ko, M. S. Torikachvili, N. Ni, S. Nandi, J. B. Leão, S. J. Poulton, D. N. Argyriou, B. N. Harmon, R. J. McQueeney, P. C. Canfield, and A. I. Goldman, Phys. Rev. B **78**, 184517 (2008).
[16] W. Yu, A. A. Aczel, T. J. Williams, S. L. Bud'ko, N. Ni, P. C. Canfield, and G. M. Luke, Phys. Rev. B **79**, 020511 (2009).
[17] M. Rotter, M. Pangerl, M. Tegel, and D. Johrendt, Angew. Chem., Int. Ed. **47**, 7949 (2008).
[18] K. Sasmal, B. Lv, B. Lorenz, A. M. Guloy, F. Chen, Y.-Y. Xue, and C.-W. Chu, Phys. Rev. Lett. **101**, 107007 (2008).
[19] H. Chen, Y. Ren, Y. Qiu, W. Bao, R. H. Liu, G. Wu, T. Wu, Y. L. Xie, X. F. Wang, Q. Huang, and X. H. Chen, Europhys. Lett. **85**, 17006 (2009).
[20] F. F. Tafti, A. Juneau-Fecteau, M.-E. Delage, S. Rene de Cotret, J.-P. Reid, A. F. Wang, X.-G. Luo, X. H. Chen, N. Doiron-Leyraud, and L. Taillefer, Nat. Phys. **9**, 349 (2013).
[21] T. Terashima, K. Kihou, K. Sugii, N. Kikugawa, T. Matsumoto, S. Ishida, C.-H. Lee, A. Iyo, H. Eisaki, and S. Uji, Phys. Rev. B **89**, 134520 (2014).
[22] V. Taufour, N. Foroozani, M. A. Tanatar, J. Lim, U. Kaluarachchi, S. K. Kim, Y. Liu, T. A. Lograsso, V. G. Kogan, R. Prozorov, S. L. Bud'ko, J. S. Schilling, and P. C. Canfield, Phys. Rev. B **89**, 220509 (2014).
[23] Y. Nakajima, R. Wang, T. Metz, X. Wang, L. Wang, H. Cynn, S. T. Weir, J. R. Jeffries, and J. Paglione, Phys. Rev. B **91**, 060508 (2015).
[24] J.-J. Ying, L.-Y. Tang, V. V. Struzhkin, H.-K. Mao, A. G. Gavriliuk, A.-F. Wang, X.-H. Chen, and X.-J. Chen, arXiv:1501.00330.
[25] B. Wang, K. Matsubayashi, J. Cheng, T. Terashima, K. Kihou, S. Ishida, C.-H. Lee, A. Iyo, H. Eisaki, and Y. Uwatoko, Phys. Rev. B **94**, 020502 (2016).
[26] D. Guterding, S. Backes, H. O. Jeschke, and R. Valentí, Phys. Rev. B **91**, 140503 (2015).
[27] A. Iyo, K. Kawashima, T. Kinjo, T. Nishio, S. Ishida, H. Fujihisa, Y. Gotoh, K. Kihou, H. Eisaki, and Y. Yoshida, J. Am. Chem. Soc. **138**, 3410 (2016).
[28] D. M. Wang, X. C. Shangguan, J. B. He, L. X. Zhao, Y. J. Long, P. P. Wang, and L. Wang, J. Supercond. Novel Magn. **26**, 2121 (2013).
[29] W. R. Meier, T. Kong, U. S. Kaluarachchi, V. Taufour, N. H. Jo, G. Drachuck, A. E. Böhmer, S. M. Saunders, A. Sapkota, A. Kreyssig, M. A. Tanatar, R. Prozorov, A. I. Goldman, F. F. Balakirev, A. Gurevich, S. L. Bud'ko, and P. C. Canfield, Phys. Rev. B **94**, 064501 (2016).
[30] W. R. Meier, T. Kong, S. L. Bud'ko, and P. C. Canfield, Phys. Rev. Mater. **1**, 013401 (2017).
[31] E. Colombier and D. Braithwaite, Rev. Sci. Instrum. **78**, 093903 (2007).
[32] G. J. Piermarini, S. Block, and J. Barnett, J. Appl. Phys. **44**, 5377 (1973).
[33] B. Bireckoven and J. Wittig, J. Phys. E: Sci. Instrum. **21**, 841 (1988).
[34] A. Eiling and J. S. Schilling, J. Phys. F: Met. Phys. **11**, 623 (1981).
[35] P. L. Alireza, S. Barakat, A.-M. Cumberlidge, G. Lonzarich, F. Nakamura, and Y. Maeno, J. Phys. Soc. Jpn. **76**, 216 (2007).

[36] K. Murata, K. Yokogawa, H. Yoshino, S. Klotz, P. Munsch, A. Irizawa, M. Nishiyama, K. Iizuka, T. Nanba, T. Okada, Y. Shiraga, and S. Aoyama, Rev. Sci. Instrum. **79**, 085101 (2008).

[37] G. J. Piermarini, S. Block, J. D. Barnett, and R. A. Forman, J. Appl. Phys. **46**, 2774 (1975).

[38] See Supplemental Material at http://link.aps.org/supplemental/10.1103/PhysRevB.96.140501 for further experimental and computational details.

[39] S. V. Sinogeikin, J. S. Smith, E. Rod, C. Lin, C. Kenney-Benson, and G. Shen, Rev. Sci. Instrum. **86**, 072209 (2015).

[40] G. Kresse and J. Hafner, Phys. Rev. B **47**, 558 (1993).

[41] G. Kresse and J. Furthmüller, Phys. Rev. B **54**, 11169 (1996).

[42] G. Kresse and J. Furthmüller, Comput. Mater. Sci. **6**, 15 (1996).

[43] P. E. Blöchl, Phys. Rev. B **50**, 17953 (1994).

[44] G. Kresse and D. Joubert, Phys. Rev. B **59**, 1758 (1999).

[45] M. Tomić, R. Valentí, and H. O. Jeschke, Phys. Rev. B **85**, 094105 (2012).

[46] M. Tomić, H. O. Jeschke, R. M. Fernandes, and R. Valentí, Phys. Rev. B **87**, 174503 (2013).

[47] R. S. Dhaka, R. Jiang, S. Ran, S. L. Bud'ko, P. C. Canfield, B. N. Harmon, A. Kaminski, M. Tomić, R. Valentí, and Y. Lee, Phys. Rev. B **89**, 020511 (2014).

[48] S. Ran, S. L. Bud'ko, W. E. Straszheim, J. Soh, M. G. Kim, A. Kreyssig, A. I. Goldman, and P. C. Canfield, Phys. Rev. B **85**, 224528 (2012).

[49] E. Gati, S. Köhler, D. Guterding, B. Wolf, S. Knöner, S. Ran, S. L. Bud'ko, P. C. Canfield, and M. Lang, Phys. Rev. B **86**, 220511 (2012).

[50] A. I. Goldman, A. Kreyssig, K. Prokeš, D. K. Pratt, D. N. Argyriou, J. W. Lynn, S. Nandi, S. A. J. Kimber, Y. Chen, Y. B. Lee, G. Samolyuk, J. B. Leão, S. J. Poulton, S. L. Bud'ko, N. Ni, P. C. Canfield, B. N. Harmon, and R. J. McQueeney, Phys. Rev. B **79**, 024513 (2009).

[51] W. Uhoya, A. Stemshorn, G. Tsoi, Y. K. Vohra, A. S. Sefat, B. C. Sales, K. M. Hope, and S. T. Weir, Phys. Rev. B **82**, 144118 (2010).

[52] R. Mittal, S. K. Mishra, S. L. Chaplot, S. V. Ovsyannikov, E. Greenberg, D. M. Trots, L. Dubrovinsky, Y. Su, T. Brueckel, S. Matsuishi, H. Hosono, and G. Garbarino, Phys. Rev. B **83**, 054503 (2011).

[53] Z. Yu, L. Wang, L. Wang, H. Liu, J. Zhao, C. Li, S. Sinogeikin, W. Wu, J. Luo, N. Wang, K. Yang, Y. Zhao, and H.-k. Mao, Sci. Rep. **4**, 7172 (2014).

[54] W. Uhoya, G. Tsoi, Y. K. Vohra, M. A. McGuire, A. S. Sefat, B. C. Sales, D. Mandrus, and S. T. Weir, J. Phys.: Condens. Matter **22**, 292202 (2010).

[55] W. O. Uhoya, G. M. Tsoi, Y. K. Vohra, M. A. McGuire, and A. S. Sefat, J. Phys.: Condens. Matter **23**, 365703 (2011).

[56] W. O. Uhoya, J. M. Montgomery, G. M. Tsoi, Y. K. Vohra, M. A. McGuire, A. S. Sefat, B. C. Sales, and S. T. Weir, J. Phys.: Condens. Matter **23**, 122201 (2011).

[57] https://github.com/danielguterding/fplowannierdensity.